NUCLEAR SCIENCE AND TECHNIQUES **25**, 060202 (2014)

An industrial CT system for monitoring a running aero-engine*

CHANG Ming (常铭),[1,2] XIAO Yong-Shun (肖永顺),[1,2] and CHEN Zhi-Qiang (陈志强)[1,2,†]

[1]*Department of Engineering Physics, Tsinghua University, Beijing 100084, China*
[2]*Key Laboratory of Particle & Radiation Imaging, Tsinghua University, Beijing 100084, China*

(Received March 17, 2014; accepted in revised form May 12, 2014; published online December 9, 2014)

In order to improve aerodynamic performance and efficiency, monitoring the geometry and position information of the internal structure with the aero-engine under various operational statuses is an important task. In this paper, a novel design of industrial computed tomography (ICT) system with a linac as X-ray source is proposed to complete the task. The major advantage of the proposed system is that it can provide visualized images of internal structures of the running aero-engine without physical disturbance, which makes it possible to extract the accurate geometry information. The main idea behind this design is to measure the projection data from various views for reconstructions making use of the rotations of the aero-engine blades, instead of the mechanical rotations in the conventional ICT system. However, due to high speed rotation of the aero-engine blades, the system faces more challenges than conventional ICT systems both in data acquisitions and reconstruction algorithms. The challenges and corresponding solutions are presented in this paper. In conclusion, the proposed ICT system provides a powerful tool for monitoring the running aero-engines.

Keywords: Dynamic imaging, Computed tomography, System design, Image reconstruction

DOI: 10.13538/j.1001-8042/nst.25.060202

I. INTRODUCTION

In aero-engine structure design and fabrication, running aero-engine test is an important experiment to improve the efficiency, aerodynamic performance and aircraft safety. For example, tip clearance has been a technical challenge in the aero-engine development. A 1% increase in tip clearance of the compressor casing will decrease the compressor efficiency by 1–3% [1], while probability of friction or collision between blade and casing increases with a too small tip clearance, causing eventually serious accidents. Also, the blade dimensions affect greatly the engine aerodynamic performance. So, it is of great significance to monitor internal geometry information of an aero-engine under various operation conditions. However, it is a harsh task to measure the inner structure under high temperature, high pressure and high rotating speed (10 000 rpm or higher) with conventional methods. For example, measurement accuracy of optical sensors can be reduced by oil dirt contamination [2], and eddy current measurement is restricted by the high temperature of aero-engines [3]. Also, it is not convenient or permissible to set up detectors or sensors in the aero-engines because they will disturb the airflow distributions.

Currently, changes in dimensions of the blades under various operating conditions are checked by indirect measurements, which cannot give a visualized image; or computer simulation, which cannot accurately simulate the complicated real working environment. X-ray computed tomography provides accurate images without physical disturbance to the object being inspected, and is suitable to monitor the running aero-engine blades [4]. Another inherent advantage of X-ray process tomography is hard-field character of X-ray, which makes it possible to achieve clear images without blurs or artifacts. Hampel *et al*. developed a gamma-ray tomography system to measure fluid distributions of a rapid rotating fluid coupling [5]. They designed an angle synchronized trigger device to sort the projection data acquired from their system [6]. They succeed in revealing fluid structure of the coupling under different rotating speeds. However, an aero-engine is much more massive and complicated than that fluid coupling, and the numerous pipelines in the stationary parts shall introduce significant contaminations to projections of the blades in high speed rotation. Also, determinations of the projection angles and suppressions of the motion blurs are challenges to the X-ray tomography because the blades rotate much faster than the fluid coupling.

In this paper, an innovative design of industrial computed tomography (ICT) system is proposed for monitoring changes in internal structure of a running aero-engine. It shall make it possible to obtain accurate images of the internal structures under different operational statuses of the aero-engine. It has the potential to derive tomographic information about the whole engine running test. In Section II, details about the system design are presented. Three major challenges to the ICT system are analyzed and feasible solutions are proposed in Section III. In Section IV, we demonstrate feasibility of the ICT system and effectiveness of the solutions through computer simulations and experiments. Finally, a conclusion is given for the proposed ICT system and the major challenges.

II. METHODS

A. System design

Different from a static scanning object in a conventional ICT system, the aero-engine blades are rotating rapidly in the

* Supported by the Transportation Construction Science and Technology Project (No. 201332849A090)
† Corresponding author, czq@mail.tsinghua.edu.cn

process of measurements. An ICT system is developed to acquire images of rotating blades under steady operating state of an aero-engine. The main idea is to measure the projection data by using the blade rotation of an aero-engine with stationary X-ray source and detector array [7, 8], rather than mechanical rotations of a conventional ICT system. As shown in Fig. 1, a 4 MeV electron linac X-ray source produces a sequence of X-ray beams pulsed at $\sim 4\,\mu$s width and the blades rotate at $\sim 10\,000$ rpm. On the other side, the detector array receives the X-rays attenuated by the aero-engine. The data are transmitted to the workstation for image reconstruction. A sensor is used to monitor fluctuation of the blade rotation and the signals are used for accelerator control.

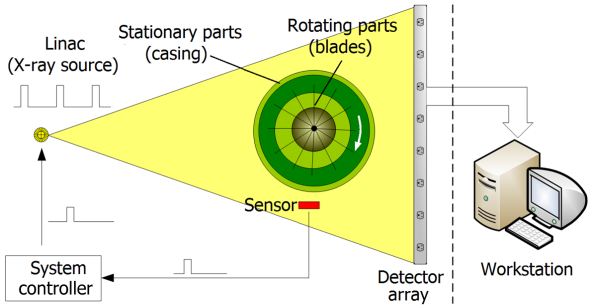

Fig. 1. (Color online) Schematic diagram of the proposed ICT system.

In conventional ICT systems, the projections from different views are acquired in step-by-step mechanical turntable rotates of the CT system. The linac is triggered according to signal of angle encoders. However, in this design, it is the object that rotates. Two trigger modes (Fig. 2), single-trigger and multi-trigger modes, are proposed. In the single-trigger mode, the linac generates a sequence of X-ray pulses with an interval of t_0 in several rotation cycles. The signals from the sensor are only used for estimating the rotation speed, but this is not necessary. This mode is more useful when the sensor signal is inexact or it is not permissible to set up such a sensor around the blades, because the trigger signal can be also sent manually. However, accuracy of the projection views is affected by the speed fluctuation in this mode. In the multi-trigger mode, the sensor sends a pulse signal to the system controller whenever a blade passes by. The accelerator is synchronized to the blade rotations. Particularly, the controller make the linac triggered with a proper delay of t_n and a period of T_{period} according to the rotation speed and ideal projection angles. A programmable logical controller (PLC) is used to achieve this function. In this mode, uniform samplings are available even though the rotation speed is not constant, because the controller adjusts the delay time t_n according to the speed fluctuation.

B. Reconstruction algorithm

The dynamic measurement procedure and the rotating blades make the recovery of the internal structure more complex and difficult. There are three major obstacles to overcome. First, it is crucial to sort the projections with corresponding projection views and ensure quality of the reconstructed image. Next, the "blocked projections" must be corrected. As all projections are acquired by using the rotating blades, the stationary casing and pipelines around the blades manifest as block contaminations in the projection data, which brings significant artifacts in the final results. Finally, there are the motion artifacts. Due to the high rotation speed, the blades rotate a certain angle in an X-ray exposure, hence the blurred edges. In the following sections, the three challenges will be analyzed.

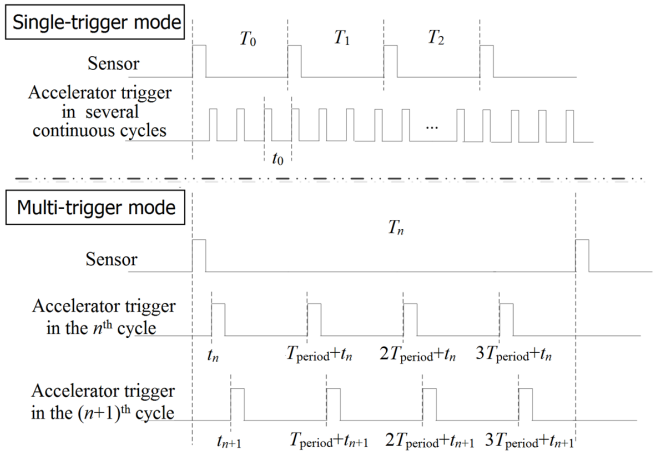

Fig. 2. (Color online) The sequence diagram of the two trigger mode: single-trigger and multi-trigger mode ($M = 4$ pulses in each cycle).

1. *Determination of projection views*

In conventional ICT systems, the exact projection views can be achieved from the angle encoder set up on the mechanical turntable. However, in this design, the angle sampling interval is determined by the product of rotation speed and the time interval between two adjacent X-ray pulses. Determination of the exact projection angles is the key to achieving high quality images. In the single-trigger mode, the linac produces pulsed X-ray beams in a given frequency. The sampling angle can be estimated according to the accelerator frequency and blade rotation speed if the latter is constant. However, due to fluctuation of the rotation speed, the projection angles are often slightly inaccurate and the errors accumulated in measurements of several rotation cycles would eventually lead to obvious stripe artifacts in the reconstructed images. In order to reduce the accumulated errors, a posterior correction-based method with statistical properties of the projections is proposed to solve the problem. The projections measured from the same view or two views quite close to each other should have a very high similarity. The similarity can be measured by cross-correlation coefficient or by standard deviation. For example, in the single-trigger mode, after M rotating cycles, the N^{th} X-ray pulse is produced when the blades rotate to the

same position where the accelerator generates the 1st X-ray pulse. Then the projection must be quite similar to the 1st projection and the angle sampling interval θ_0 can be estimated by Eq. (1) and the n^{th} projection views can be calculated by Eq. (2).

$$\theta_0 = 360M/N, \tag{1}$$

$$\theta_n = (n-1)\theta_0. \tag{2}$$

From Eq. (2), the error of projection views increases with n. In order to suppress the accumulated errors, adjacent projections are grouped and the projections are divided into several groups. Then images are reconstructed with these projections, respectively. While limited amount of projections suppresses the accumulating errors, insufficient projection data may affect the image qualities. For taking full use of all the projections, registrations between these pre-reconstructed images are done to acquire the relations of projection angles (offset angles) among different projection groups. Finally, all the projection data are reorganized for reconstructions while the accumulating errors are greatly limited. The complete work flow is presented in Fig. 3.

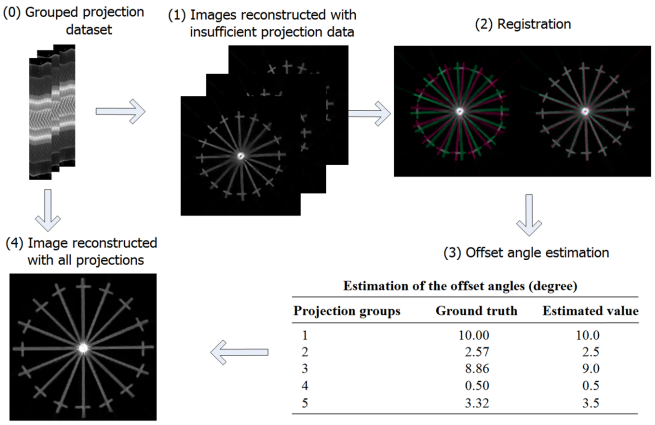

Estimation of the offset angles (degree)

Projection groups	Ground truth	Estimated value
1	10.00	10.0
2	2.57	2.5
3	8.86	9.0
4	0.50	0.5
5	3.32	3.5

Fig. 3. (Color online) Work flow of the posterior correction based method. The scale bar is set to [0.0 1.0].

With a sensor to detect the blades, the multi-trigger mode can be adopted, and uniform angle samplings can be achieved by the controller, in which a PLC adjusts the delay time and pulse frequency adaptively to match the changing rotation speed. Projection views incorporating information from the sensor are more accurate. If the speed change is too big, the projections obtained far from the ideal positions can be removed or re-measured.

2. *Correction of blocked projections*

The block contaminations in the projections data are caused by the stationary casing and complicated pipelines around the blades. It is noted, however, that both of the source-detector and block parts keep static in the whole scanning procedure, which means that the block components to a specific detector at different views are constant. The expression of discrete imaging model at i^{th} projection view to the j^{th} detector can be given as

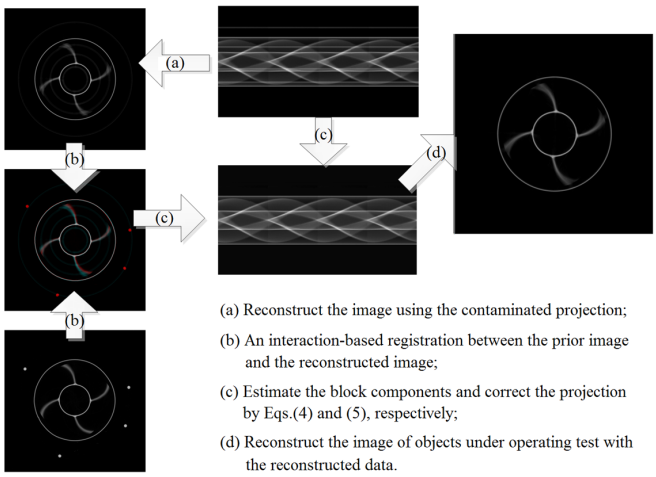

Fig. 4. (Color online) Work flow of the interaction based method with a prior image. The scale bar is set to [0.0 0.04].

$$H_{i,j}f + b_j = p_{i,j}, \tag{3}$$

where H is the projection operator, f is the image datum, b is the block term, and p is the projection datum. Details of the reconstructed image using the contaminated projections are seriously corrupted by these artifacts, making it hard to determine the blade edges.

An interaction-based method with a prior image is developed to address the problem. Contributions of the block components from the acquired projection data will be removed, or they will be estimated. In this paper, a prior image is incorporated to achieve the goal. Before the dynamic measurements, a static aero-engine is scanned by a conventional ICT and an image without blocks is reconstructed. This can be used as the prior image f_{prior} in the procedure. The prior image f_{prior} is used to simulate the contribution of $H_{i,j}f$ for estimating the block components though there are some differences in details. It should be noted that the registration between the reconstructed image and the prior image is essential before the estimation, because they are generally not at the same location. Some serious artifacts besides the deformations can appear in the reconstructed image, making it difficult to apply auto match technologies, such as the Scale-Invariant Feature Transform (SIFT) method [9], for the registration. Hence, an interaction is introduced into the registration procedure. Then, a forward-projection of the matched prior image $\tilde{f}_{\text{prior}}$ with the practical scanning configuration parameters is performed. The block components of j^{th} detector, $\tilde{b}_{\text{j}}$, can be estimated by

$$\tilde{b}_j = \frac{1}{N_{\text{view}}} \sum_{i=1}^{N_{\text{view}}} p_{i,j} - H_{i,j}\tilde{f}_{\text{prior}}. \tag{4}$$

By Eq. (5), the $\tilde{b}_j$ are used to obtain corrected projection data, which are used to reconstruct the final image.

$$\tilde{p}_{i,j} = p_{i,j} - \tilde{b}_j. \tag{5}$$

The summarized work flow is shown in Fig. 4.

3. *Suppression of exposure blurs*

The exposure blurs in the final reconstructed images are due to the speed high rotation, by which the blades rotate a certain angle during an X-ray exposure. This gives rise to significant degradations of the image spatial resolution and great limitations of the ICT in high-precision measurements. Therefore, the blade rotations during the X-ray exposure must be considered in the reconstruction method. An iterative reconstruction method is proposed based on the discretization of the X-ray exposure procedure. The main idea behind the method is to discrete the dynamic X-ray exposure to several virtual conventional exposure child procedures. Specifically, this physical procedure is divided into M virtual conventional static exposure processes. In different sub-processes, the blades rotate to different positions as

$$\begin{aligned} I_j = I_0 \left[\frac{1}{M}\sum_{i=1}^{M}\exp(-H_{ij}f)\right] \Rightarrow \sum_{i}^{M}\exp(-H_{ij}f) \\ = MI_j/I_0, \end{aligned} \tag{6}$$

where the subscripts j and i indicate the j^{th} X-ray path and the number of sub-process of virtual conventional static exposure, respectively. In fact, $H_{i,j}$ is the system matrix of j^{th} detectors at i^{th} sub-process.

Equation (6) is a nonlinear problem raising great challenges to the conventional reconstruction methods, where the scanned object is assumed static. Approximately, however, it can be converted to a linear problem using the Taylor expansion with a good initial guess f_0.

$$\begin{aligned} &H_j \mathrm{d}f = p_j, \\ &H_j = \sum_{i=1}^{M}[\exp(-H_{ij}f_0)H_{ij}], \\ &p_j = \sum_{i=1}^{M}\exp(-H_{ij}f_0) - \frac{MI_j}{I_0}. \end{aligned} \tag{7}$$

We note that the difference image $\mathrm{d}f$ instead of f is calculated in each iteration. Therefore, the initial guess f_0 should be updated after each iteration by $f_0 = f_0 + \mathrm{d}f$.

According to our research, the initial guesses can be from either a prior image or the blurred image. Then, it can be solved by widely used algebraic reconstruction methods only with some simple modifications on the system matrix and projection data as shown in Eq. (7).

In summary, Fig. 5 shows the total flowchart for a comprehensive demonstration of the system challenges and the corresponding solutions.

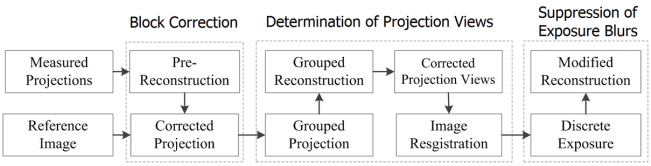

Fig. 5. The total flowchart of the system challenges and corresponding solutions.

III. SIMULATIONS AND EXPERIMENTS

A. Numerical simulations

In computer simulation, feasibility of the single-trigger mode of the proposed system was validated first. As shown in Fig. 6(a), a simple phantom is designed to simulate the aero-engine blades. The angle-intervals of samplings were estimated based on similarities of projections as mentioned above, but errors of the estimated angle-intervals were inevitable. The errors accumulated in projection angles because projection angles were calculated by accumulating the angle-intervals. As shown in Fig. 6(b), quality of the image reconstructed with rough projection angle positions degraded, which greatly influenced the following quantitative analysis. On the contrary, visible improvements in image quality were achieved using the proposed posterior correction based method. The relative error reduced to 48% of the conventional one because the maximum estimated errors of projection angles decreased to 1.61° from 4.3°. Hence, the posterior correction of projection angles is essential to guarantee the image quality in single-trigger mode when the proposed system is applied to monitor the running aero-engine blades.

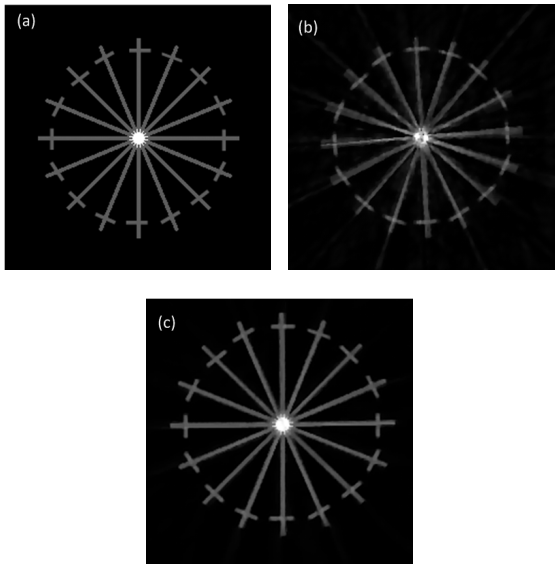

Fig. 6. Simulation results with simple phantom. (a) Original image; (b) image reconstructed with rough angle positions; (c) image reconstructed by posterior correction based method. The scale bar is set to [0.0 1.0].

Next, an air blower was used as a phantom to demonstrate the effectiveness of the method for suppressing the exposure blurs. However, air blowers rotate at about 2900 rpm, rather than 10 000 rpm of aero-engine blades. In order to simulate projections of real rotating aero-engine blades, the successive projections were accumulated to simulate significant rotating movements during the X-ray exposures. The results of conventional method and ICT are presented in Fig. 7.

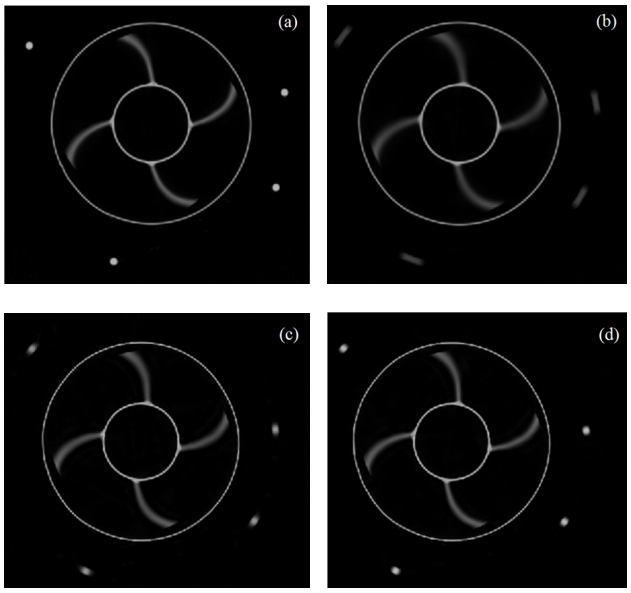

Fig. 7. Simulation with an air blower as the phantom. (a) Reference image; (b) image reconstructed by conventional method; (c) and (d) images reconstructed by our method with 8 and 16 virtual exposures, respectively. The scale bar is set to [0, 0.04].

In Fig. 7, compared with the reference image, significant exposure blurs and the decrease of contrast-to-noise ratio (CNR) can be observed in Fig. 7(b) using conventional reconstruction method due to the rotations during the X-ray exposure, while the images reconstructed by our method are of sharp edges (Figs. 7(c) and 7(d)). For quantitative analysis, the CNR at blade edges were calculated. The CNRs of Figs. 7(b), 7(c) and 7(d) were 50, 70 and 80, respectively. So, the more virtual child exposures used to simulate the actual exposure, the better result will be achieved, with heavier computations, though. In practice, the number of virtual exposures is often determined by the tradeoff between image quality and computations. The development of corresponding accelerated method using GPU will be part of future work because of its high parallelism. The high quality image makes it possible to detect minor changes in internal structure of the running aero-engine. It also demonstrates the effectiveness of our method in suppressing exposure blurs.

B. Experiments

In order to demonstrate feasibility of the proposed ICT system and effectiveness of the methods, a 2 900 rpm air blower

Fig. 8. (Color online) The air blower used in the experiment simulating the aero-engine.

was scanned. Seated on the casing, a laser sensor generated a pulse when the blade tip passed by. In order to simulate pipelines of an aero-engine, several steel columns were placed randomly around the air blower (Fig. 8). In this experiment, multi-trigger mode was adopted. The maximum frequency of the 4 MeV linac is 250 Hz, so 4 samplings were acquired in each cycle. The total 1 024 measurements were completed in 256 cycles. In other words, the whole scanning time is in less than 6 s, which is significantly faster than conventional CT measurements. It is possible to achieve several tomographic images in the test.

Firstly, a conventional ICT scan with the air blower in static was performed and internal structure of the air blower under idle state was reconstructed (Fig. 9(c)). Next, dynamic measurements were carried out with the air blower rotating at about 2 900 rpm. The internal structure was reconstructed with the reorganized projection data (Fig. 9(b)). However, some significant ring artifacts caused by the steel columns corrupted the image quality (Fig. 9(d)). Then, the projection data were corrected by using the interaction-based method with the static image as the prior image. It can be seen from Figs. 9(e) and 9(f) that the reconstructed image of blade shapes differs significantly from the prior image. So, a registration was carried out according to the major structures, such as the air blower casing. The final image (Fig. 9(g)) re-

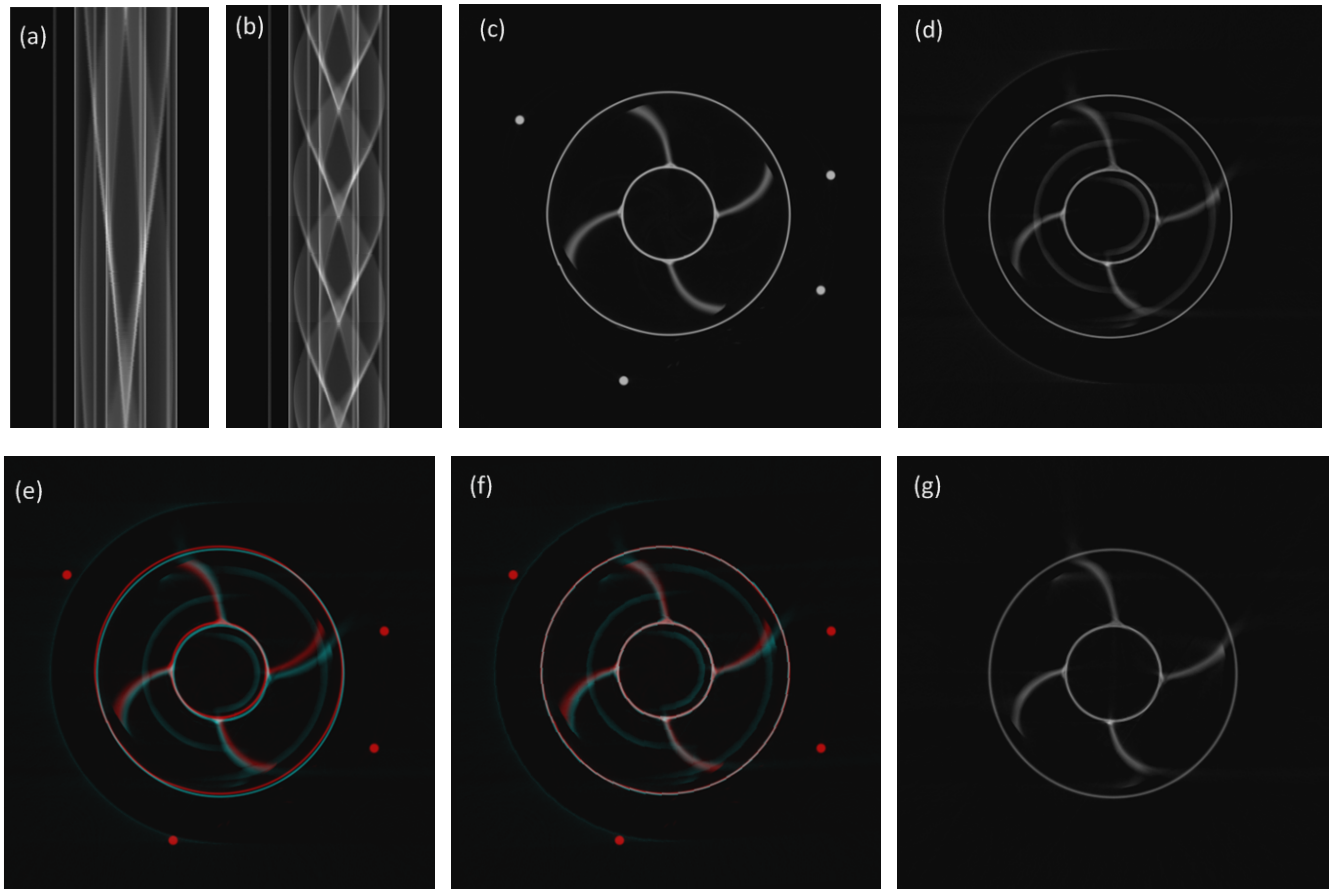

Fig. 9. (Color online) Experiment results with an air blower. (a) original sinogram; (b) reorganized sinogram; (c) reconstruction of conventional static ICT; (d) image reconstructed using the projections without correction; images ((c) in red channel and (d) in blue channel) before (e) and after (f) registration; (g) image reconstructed using the projections with correction. The scale bar is set to [0, 0.04].

constructed using the projections corrected by the interaction-based method was almost free of ring artifacts, and the main differences in blade shapes were well recovered. These improvements in the image quality are meaningful for geometric measurements. But there were still some local artifacts caused by the systematic errors, such as fluctuation of the sensor signal, mechanical vibration and some other engineering problems. The experiment design with a sensor of enhanced stability will be adjusted for further improvement of the image quality.

IV. CONCLUSION

In this paper, an innovative design of X-ray process tomography system is presented to obtain internal structure images of running aero-engine blades, which makes it possible to extract accurate geometry information of internal structures of an aero-engine under different operational statuses. Compared with conventional measurements, it has the potential to achieve high-quality image under harsh measurements without physical disturbance. The image sequence about each steady state during the running aero-engine test can be achieved by the proposed system, which is meaningful to the design and control of the aero-engine, though only certain steady state is involved in this paper. Its advantages of non-contact and visual imaging make it suitable for monitoring the internal structure changes of running aero-engines. Three major challenges caused by the dynamic measurements and rapid rotating movements are discussed. Some feasible solutions are raised in this paper and the effectiveness of these methods is demonstrated by simulating and experimental results. These basic researches are meaningful to the following system implementations in the future. Although the problem of measuring tip clearance was not solved completely, the proposed system with corresponding algorithm provides a new powerful tool based on CT technology for not only dynamic measurements of the tip clearance but also inspections of the internal geometry and position changes. Furthermore our system design and solutions are not limited to monitor running aero-engine blades. It can be also further expanded to other X-ray process tomography applications in the fields of surveying internal structure changes of rapid moving objects, such as gas turbines or steam turbines.

[1] Lattime S B and Steinetz B M. J Propul Power, 2004, **20**: 302–311.
[2] Pffister T, Buttner L,Czarske L, *et al*. Meas Sci Technol, 2006, **17**: 1693–1705.
[3] Lavagnoli S, Paniagua G, Tulkens M, *et al*. Mech Syst Signal Pr, 2012, **27**: 590–603.
[4] Xiao Y, Chen Z and Zhang L. System design and experimental research on tip clearance measurement of aero-engines by digital radiograph. The 9th International Conference on Electronic Measurement & Instruments, Beijing, China, Aug. 16–19, 2009.
[5] Hampel U, Hoppe D, Bieberle A, *et al*. J Fluid Eng-T ASME, 2008, **130**: 091402.
[6] Hampel U, Bieberle A, D. Hoppe, *et al*. Rev Sci Instrum, 2007, **78**: 103704–103704.
[7] Chang M, Xiao Y, Chen Z, *et al*. Proceeding SPIE 8506, Developments in X-Ray Tomography VIII, 2012, 85060Z.
[8] Chang M, Xiao Y, Chen Z, *et al*. IEEE Nucl Sci Conf R, 2011, 1358–1361.
[9] Lowe D G. Int J Comput Vision, 2004, **6**: 91–110.